

Voltage generation induced by mechanical straining in magnetic shape memory materials

I. Suorsa, J. Tellinen, K. Ullakko, and E. Pagounis^{a)}
AdaptaMat Ltd., Yrityspiha 5, 00390 Helsinki, Finland

(Received 12 December 2003; accepted 1 March 2004)

Magnetic shape memory (MSM) materials change their shape with the magnetic field. They can also be used in the reverse operation as sensors or voltage generators. The present paper demonstrates that large voltages are induced when the MSM material is mechanically compressed inside a MSM actuator. The experimental results reveal that voltages of close to 100 V were generated with a Ni–Mn–Ga MSM material subjected to short mechanical impulses, because of a change in its magnetization. The induced voltage depends on the geometrical and material parameters of the MSM actuator, as well as on the speed by which the MSM material changes its shape. A magnetic model for calculating the induced voltage is proposed and the measurement results from a MSM-type actuator are presented. The magnetic model demonstrates good accordance with the experimental results. The physical reason for the voltage signal is discussed and potential applications are proposed. © 2004 American Institute of Physics. [DOI: 10.1063/1.1711181]

I. INTRODUCTION

Magnetic shape memory (MSM) are a class of smart materials that change their shape when exposed to a moderate magnetic field.^{1–6} The advantage of MSM compared to currently available smart materials (piezoceramics, thermal shape memory, magnetostrictive alloys) is their ability to generate up to 10% strains at frequencies well above 100 Hz.⁷ The MSM mechanism is based on the martensite twin boundary motion driven by the external magnetic field, when the material is in complete martensite state. The martensite crystal, after transformation from cubic austenite, consists of the mixture of tetragonal martensite variants, having different *c*-axis orientation, separated by twin boundaries. When the MSM material is exposed to an external magnetic field the twins in a favorable orientation relative to the field direction grow at the expense of other twins. Magnetic field *H* increases the amount of twin variants of “preferable” orientation relative to the field, i.e., the twin boundaries move in the material. For the time being, the MSM effect was observed in Ni₂MnGa, Fe–Pd, and Co–Ni–Al alloys. Among them, the near stoichiometric Ni₂MnGa alloy has shown the best stroke performance and is considered in the present work.

Because of their large energy output, MSM materials show enormous potential in high-stroke, dynamic actuator applications. On the other hand, when the material is subjected to mechanical straining the twin variants reorient, too, which alters their magnetization and the surrounding magnetic field. This phenomenon can be used for sensor applications and for voltage generation. For the time being, only little work has been performed on the inverse (sensor) MSM effect,⁸ and no published report has demonstrated voltage generation using MSM materials. In the present study, a

MSM actuator is used to demonstrate voltage generation induced by mechanical straining of the MSM material. A model of the magnetic circuit diagram of the actuator is given, and theoretical results are calculated and compared with the measured ones. Also the relationship between the induced voltage and the speed by which the MSM material changes its shape is studied, for possible applications in speed sensors.

II. MAGNETIC MODELING OF MSM MATERIALS

The MSM material consists of internal areas, twin variants, which are magnetically anisotropic. The MSM effect is based on changing the proportions of these variants by the magnetic field.^{9,10} Because of the different twin variants the magnetic properties of the MSM material vary locally. On the other hand, for calculation purposes, it is beneficial to model the material as a homogeneous object. To take different areas into account we use effective magnetic properties to describe the magnetic field variables. These are the effective field strength H_{MSM} , and the effective flux density B_{MSM} . We define these as average values of the field inside the MSM material.

The effective $B_{\text{MSM}}-H_{\text{MSM}}$ magnetization curve of the MSM material depends on its strain state. A linear dependence between the magnetization, the magnetic flux density, and the strain ϵ of the MSM material has been proposed,¹¹

$$B_{\text{MSM}}(H_{\text{MSM}}) = B_t(H_{\text{MSM}}) + \frac{\epsilon}{\epsilon_{\text{max}}} [B_a(H_{\text{MSM}}) - B_t(H_{\text{MSM}})], \quad (1)$$

where $B_t(H_{\text{MSM}})$ is the flux density along the hard magnetization direction, $B_a(H_{\text{MSM}})$ is the flux density along the easy magnetization direction, and ϵ_{max} is the maximum strain. Equation (1) represents the situation where the magnetic reluctances of the variants are considered to be magnetically

^{a)}Electronic mail: pagounis@adaptamat.com

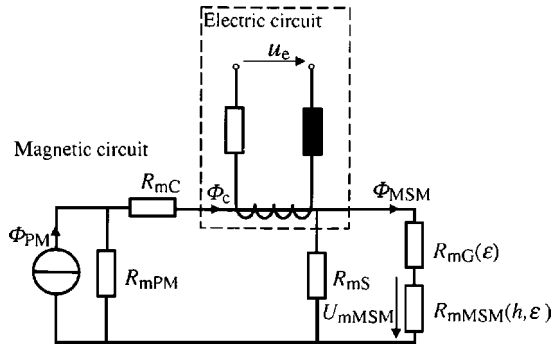


FIG. 1. The magnetic circuit diagram of the MSM actuator with biasing permanent magnets.

parallel to each other. The other extreme is the case when the variants are magnetically in series. In this case the effective magnetization curve of the MSM material is defined by

$$H_{MSM}(B_{MSM}) = H_t(B_{MSM}) + \frac{\epsilon}{\epsilon_{max}} [H_a(B_{MSM}) - H_t(B_{MSM})], \quad (2)$$

where the $H_t(B_{MSM})$ is the field strength along the hard magnetization direction and $H_a(B_{MSM})$ is the field strength along the easy magnetization direction of the MSM material. Accordingly, the curve $H_t(B_{MSM})$ is an inverse function of the $B_t(H_{MSM})$, while the curve $H_a(B_{MSM})$ is an inverse function of the $B_a(H_{MSM})$.

III. THE MAGNETIC CIRCUIT OF A MSM ACTUATOR

In the present study a MSM actuator was used to measure the induced voltages when the shape of the MSM material inside the actuator is changed. In order to model the induced voltages one has to look into the electric and magnetic properties of the MSM actuator. The actuator consists of coils to produce the magnetic field, ferromagnetic core to increase the field, and the MSM material to generate the mechanical motion.¹² The MSM material is placed in an air-gap within the actuator's core. In addition, biasing permanent magnets are used to generate a dc field. Accordingly, the MSM actuator can be represented by the simplified equivalent electric and magnetic circuit diagram given in Fig. 1. In this modeling diagram we neglect the effect of the eddy currents and saturation or hysteresis effects in the magnetic circuit of the actuator.

In Fig. 1 the Φ_{PM} is the magnetic flux generated with the permanent magnets, which is constant. The R_{mPM} represents the reluctance of the biasing air gap, R_{mC} is the reluctance of the core, R_{mS} is the reluctance of the stray field passing the MSM material, R_{mG} is the reluctance of the air gap between the MSM material and the core, and R_{mMSM} is the reluctance of the MSM material. Because the MSM material changes its shape, the air gap and the material's width are changing. Therefore, the R_{mG} and the R_{mMSM} depend on the strain state of the MSM material. In addition, the R_{mMSM} depends also on the magnetic field inside the MSM material (H_{MSM}, B_{MSM}). These two reluctances can be written as

$$R_{mG}(\epsilon) = \frac{R_{mG}(\epsilon=0)}{x_{G0}} (x_{G0} + \epsilon x_{MSM0}) \quad (3)$$

and

$$R_{mMSM}(\epsilon, H_{MSM}, B_{MSM}) = R_{mMSM}(\epsilon=0, H_{MSM}, B_{MSM})(1 - \epsilon), \quad (4)$$

where x_{G0} is the air-gap width between the MSM material and the ferromagnetic core, and x_{MSM0} is the MSM material width, when the strain $\epsilon=0$. It follows from the equivalent circuit of Fig. 1 that the flux $\Phi_{MSM} = B_{MSM}A_{MSM}$ and magnetic voltage $U_{mMSM} = H_{MSM}x_{MSM}$ are correlated. When the current in the coils is $i=0$, the relation becomes

$$B_{MSM}A_{MSM} = \frac{R_{mPM}\Phi_{PM}}{R_{m1}} - \frac{x_{MSM}H_{MSM}}{R_{m2}}, \quad (5)$$

where A_{MSM} is the cross-section area of the MSM material, x_{MSM} is the width of the MSM material, and

$$R_{m1} = R_{mPM} + R_{mC} + R_{mG} + \frac{R_{mG}}{R_{mS}} (R_{mPM} + R_{mC}) \quad (6)$$

and

$$R_{m2} = R_{mG} + \frac{(R_{mPM} + R_{mC})R_{mS}}{R_{mS} + R_{mPM} + R_{mC}}. \quad (7)$$

From the circuit diagram given in Fig. 1 one can calculate the magnetic flux going through the coils as

$$\Phi_c = \frac{R_{mPM}\Phi_{PM}}{R_{mPM} + R_{mC} + \frac{(R_{mG} + R_{mMSM})R_{mS}}{R_{mG} + R_{mMSM} + R_{mS}}}. \quad (8)$$

When external mechanical force is applied on the MSM material, its shape changes, and R_{mMSM} changes as well. Accordingly, the coil flux Φ_c changes and induces the voltage u_e in the winding. The instant value of the induced voltage u_e is defined by the differential equation:

$$u_e = N \frac{d\Phi_c}{dt} = \frac{N}{l_{MSM}} \frac{d\Phi_c}{d\epsilon} \nu, \quad (9)$$

where N is the number of the coil turns, l_{MSM} is the length of the MSM element, t is the time, and ν is the speed by which the MSM material changes its shape. Therefore, the induced voltage depends on the geometrical and material parameters of the MSM actuator, as well as on the speed of the MSM material. We assume the speed ν as the speed of the upper end of the MSM material.

In order to calculate the induced voltage using Eq. (9) one has to calculate the magnetic reluctance R_{mMSM} . Accordingly, the magnetic fields (H_{MSM}, B_{MSM}) have to be determined. Equation (1) or (2) together with Eq. (5) can be used for this purpose. In Fig. 2 a graphical solution of the problem is presented. The figure presents the magnetization curves of the MSM material along the easy and the hard direction, as well as one effective magnetization curve. Also the curve representing Eq. (5) is visible. Even though the reluctance R_{mG} and the width x_{MSM} depend on the strain ϵ the curve is close to linear. In Fig. 2 the crossing point of the

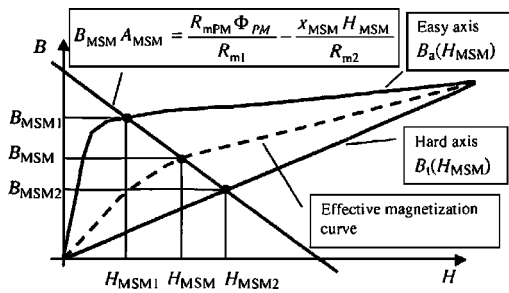


FIG. 2. The magnetization curves $B_e(H_{MSM})$, $B_h(H_{MSM})$ and one effective magnetization curve of the MSM material. The curve derived from Eq. (5) is also shown.

magnetization curve and the curve representing the magnetic circuit [Eq. (5)] gives the magnetic field solution (H_{MSM} , B_{MSM}).

The initial point (H_{MSM1} , B_{MSM1}) in Fig. 2 represents the fully expanded MSM material. In this case, the permeability of the MSM material has its maximum value and the magnetic reluctance R_{mMSM} has its minimum value. Accordingly, the magnetization curve is along the easy axis. When a compression force is applied the magnetic properties of the MSM material change, and the dashed line in Fig. 2 represents the effective magnetization curve (permeability decreases and magnetic reluctance increases). Therefore, the flux in the actuator core Φ_c decreases and induces the voltage u_e in the winding. When the material is fully compressed, the operating point moves to (H_{MSM2} , B_{MSM2}), where the magnetization curve corresponds to the hard axis. At this point the MSM material has the minimum permeability, the magnetic reluctance R_{mMSM} has its maximum value, and the magnetic flux Φ_c has its minimum value. When the MSM material expands the value of the magnetic flux Φ_c increases and the process follows the opposite direction to the initial point (H_{MSM1} , B_{MSM1}).

IV. MATERIALS AND EXPERIMENTAL PROCEDURES

A prototype MSM actuator was used to demonstrate the voltage generation. The actuator specifications can be seen in Table I. The actuator's core was made from laminated iron and the coil from round copper wire. The MSM material in the actuator was non-stoichiometric Ni_2MnGa alloy with the chemical composition of (wt %) Ni49–Mn26–Ga25.

The MSM material in the actuator was elongated magnetically and then exposed to short mechanical impulses, causing it to compress. The voltage induced in the coils and the strain state of the MSM element were recorded. The measurement setup can be seen in Fig. 3. The shape change of the MSM element was recorded with optoNCDT 1800 laser displacement sensor (Micro-Epsilon GmbH & Co KG),

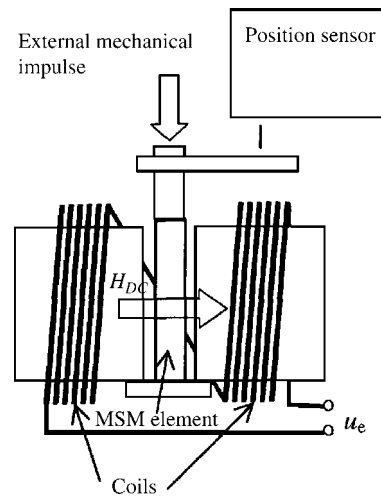


FIG. 3. Measurement setup of the MSM actuator.

which has the accuracy of $2 \mu\text{m}$ and the sampling frequency of 0.2 ms. The induced voltages were measured with HP 54603B oscilloscope.

V. RESULTS AND DISCUSSION

Based on the geometry of the MSM actuator the parameters of the magnetic circuit used in Eqs. (3)–(8) can be derived. These are summarized in Table II. On the other hand, the values of R_{mG} were calculated using Eq. (3). The reluctance R_{mMSM} was calculated by solving the magnetic fields (H_{MSM} , B_{MSM}) and using Eq. (4) for the strain dependence.

The measured voltage and strain change of the MSM material, as well as the calculated voltages, are summarized in Fig. 4. The calculated voltage values were derived from Eq. (9), using the measured strain changes and Eq. (2) for the effective magnetization curve. Figure 4 demonstrates that the calculated voltages are in good accordance with the measured ones. On the other hand, it is seen that the peak value of the calculated induced voltage is higher, 94 V, than the measured value, which is 63 V. When the magnetization curve was calculated using Eq. (1), the calculated peak voltage was even higher (116 V).

The measured and the calculated flux densities were also compared. The measured flux density in the core was derived by integrating the induced voltage. The integration was performed using the voltage curve of Fig. 4. The measured values are summarized in Fig. 5, together with the calculated ones. The effective magnetization curve was calculated using Eqs. (1) and (2). When Eq. (2) is used the measured values are in good accordance with the calculated ones. On the

TABLE I. Material and geometrical parameters of the MSM actuator.

Resistance of coils	159 Ω
Inductance of coils	6.98 H
Number of turns in coils	4000
Size of MSM element	5 mm \times 0.3 mm \times 17 mm
Size of the actuator	20 mm \times 30 mm \times 123 mm

TABLE II. Parameters used in the magnetic circuit of Fig. 1.

Φ_{PM}	0.26 mWb
R_{mPM}	$0.228 \times 10^6 \text{ A}/(\text{T} \times \text{m}^2)$
R_{mC}	$0.352 \times 10^6 \text{ A}/(\text{T} \times \text{m}^2)$
R_{mS}	$7.520 \times 10^6 \text{ A}/(\text{T} \times \text{m}^2)$
$R_{mG} (\epsilon = 0)$	$0.562 \times 10^6 \text{ A}/(\text{T} \times \text{m}^2)$

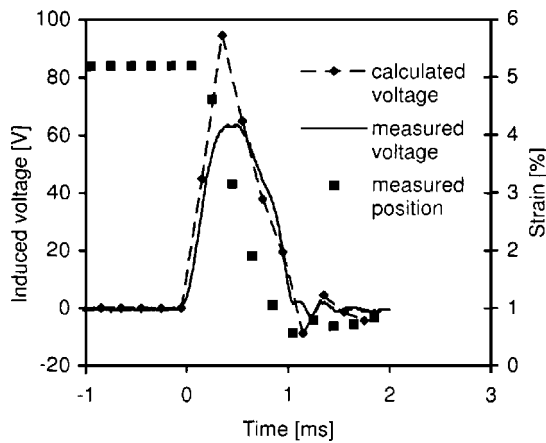


FIG. 4. Position and induced voltages when the MSM material is mechanically compressed. The induced voltage calculated using Eqs. (2) and (9) is also presented.

other hand, less accurate results were derived using Eq. (1), where the difference with the measured results was as large as 0.043 T (29%).

Figure 6 presents the modeled magnetic fields (B_{MSM}, H_{MSM}) in the MSM material during the testing. The curves are calculated using Eq. (5) and Eq. (1) or (2). Due to the different magnetization assumption (magnetic reluctances of the variants are considered magnetically in parallel and in series, respectively) the curves are not overlapping, and their start and end points are not the same. The easy and hard magnetization curves of the MSM material used in the calculations are also visible in Fig. 6.

In the present model, the dependence of the effective permeability on the strain of the MSM material is of prime importance. This is particularly true when the induced voltage depends on the derivative of the effective permeability of the MSM material. Error can also be caused by the actuator dimension inaccuracies, especially in the air gaps, where small variations can influence the model results significantly. Besides the modeling sensitivity to input parameters, the neglected eddy currents can be an error source, too. The induced voltages are high and they are generated fast, which

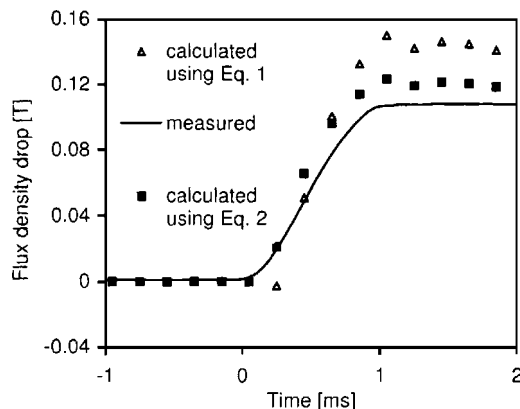


FIG. 5. Measured and calculated flux density reduction in the actuator core when the MSM material is compressed. The calculated values were derived using Eq. (9) together with Eq. (1) or (2).

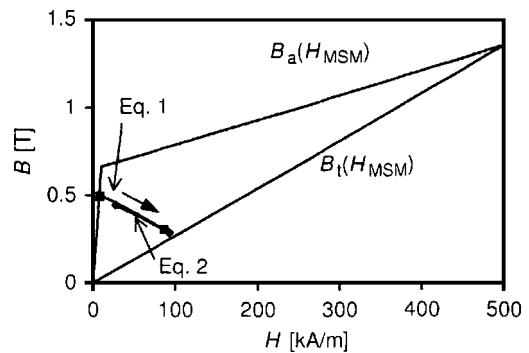


FIG. 6. Calculated $B-H$ curves derived from Eq. (5) together with Eqs. (1) and (2). The magnetization $B-H$ curves used in the calculation are visible, too.

gives rise to significant eddy currents in the whole magnetic circuit, influencing, thus, the measured voltages.

The relationship between the speed of the MSM material and the induced voltage was also studied. The speed was calculated from the strain curve of Fig. 4. In Fig. 7 the measured induced voltages and the speed of the MSM material are presented. It is seen that the induced voltage follows the speed, i.e., the relationship is similar to that derived from Eq. (9).

The measured peak induced voltages as a function of the peak speed are summarized in Fig. 8. Based on Eq. (9) the result should be linear or close to linear. Nonlinearity to the formula is caused by the derivative of the flux, which is nonconstantly dependent on the strain of the material. As can be seen in Fig. 8, the results do indeed form a line, which is in accordance with the theory. On the other hand, the quantitative results, derived from Eq. (9), give considerably higher values, compared with the measured slope in Fig. 8. The measured slope is 44.5 V s/m, while the calculated slope is 102 V s/m, using Eq. 1 ($\epsilon=0.03$), and 65 V s/m using Eq. 2 ($\epsilon=0.03$).

VI. CONCLUSIONS

The reverse MSM effect was studied and was used in voltage generation. When the MSM material is subjected to short mechanical impulses its magnetization changes. In the present study this effect was used to generate voltage using a Ni-Mn-Ga MSM material placed inside a biased MSM ac-

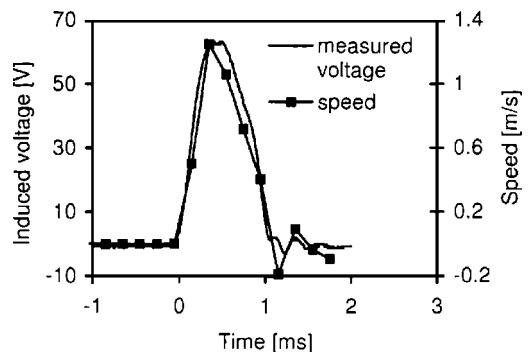


FIG. 7. Induced voltage and speed of the MSM material subjected to mechanical impulses.

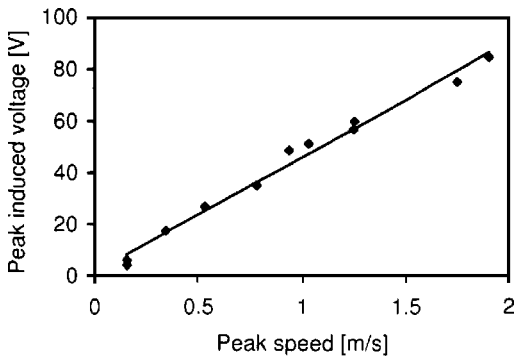


FIG. 8. Measured peak induced voltages as a function of the MSM material's peak speed.

tuator. The measured induced voltages were large, even in this nonoptimized and small measurement system, and reached values close to 100 V. The induced voltage depends on the geometrical and material parameters of the MSM actuator, as well as on the speed by which the MSM material changes its shape.

Based on the MSM effect and the actuator structure a model to calculate the induced voltages was developed. The results calculated from the model were compared with the

experimental ones. Generally, the modeling of the induced voltages has difficulties, due to the strong sensitivity to input parameters. However, in the present study the modeling results demonstrated good accordance with the measurements. The described method and system can be used in voltage or power generation. In addition, the induced voltages were proportional to the speed of the MSM material, thus, the device can also be used as a speed sensor.

¹K. Ullakko, J. K. Huang, C. Kantner, R. C. O'Handley, and V. V. Kokorin, *Appl. Phys. Lett.* **69**, 1966 (1996).

²S. J. Murray, M. Marioni, S. M. Allen, and R. C. O'Handley, *Appl. Phys. Lett.* **77**, 886 (2000).

³R. D. James, R. Tickle, and M. Wuttig, *Mater. Sci. Eng., A* **273–275**, 320 (1999).

⁴J. M. McLaren, *J. Appl. Phys.* **91**, 7801 (2002).

⁵D. I. Paul, J. Marquiss, and D. Quattrochi, *J. Appl. Phys.* **93**, 4561 (2003).

⁶A. Sozinov, A. A. Likhachev, N. Lanska, and K. Ullakko, *Appl. Phys. Lett.* **80**, 1746 (2002).

⁷I. Suorsa, J. Tellinen, E. Pagounis, I. Aaltio, and K. Ullakko, in *Proceedings ACTUATOR 2002, Eighth International Conference on New Actuators*, Bremen, Germany, June 2002, p. 158.

⁸P. Muellner, V. A. Chernenko, and G. Kostorz, *Scr. Mater.* **49**, 129 (2003).

⁹R. C. O'Handley, *J. Appl. Phys.* **83**, 3263 (1998).

¹⁰A. Likhachev and K. Ullakko, *Phys. Lett. A* **275**, 142 (2000).

¹¹A. Likhachev and K. Ullakko, *Eur. Phys. J. B* **14**, 263 (2000).

¹²J. Tellinen, I. Suorsa, A. Jääskeläinen, I. Aaltio, and K. Ullakko, in *Proceedings ACTUATOR 2002, Eighth International Conference on New Actuators*, Bremen, Germany, June 2002, p. 566.